



Published in final edited form as:

Neuroimage. 2008 August 15; 42(2): 1032–1044. doi:10.1016/j.neuroimage.2008.03.057.

COGNITIVE PROCESSING SPEED AND THE STRUCTURE OF WHITE MATTER PATHWAYS: CONVERGENT EVIDENCE FROM NORMAL VARIATION AND LESION STUDIES

And U. Turken^{1,2}, Susan Whitfield-Gabrieli^{1,3}, Roland Bammer⁴, Juliana Baldo⁵, Nina F. Dronkers^{5,6}, and John D. E. Gabrieli^{1,3,4}

¹Department of Psychology, Stanford University, Stanford, CA 94305

⁴Department of Radiology, Stanford Medical School, Stanford, CA 94305

⁵Center for Aphasia and Related Disorders, Veterans Affairs Northern California Health Care System, Martinez, CA 94553

⁶Neurology Department, University of California, Davis, Davis, CA 95616

Abstract

We investigated the relation between cognitive processing speed and structural properties of white matter pathways via convergent imaging studies in healthy and brain-injured groups. Voxel-based morphometry (VBM) was applied to diffusion tensor imaging data from thirty-nine young healthy subjects in order to investigate the relation between processing speed, as assessed with the Digit-Symbol subtest from WAIS-III, and fractional anisotropy, an index of microstructural organization of white matter. Digit-Symbol performance was positively correlated with fractional anisotropy of white matter in the parietal and temporal lobes bilaterally and in the left middle frontal gyrus. Fiber tractography indicated that these regions are consistent with the trajectories of the superior and inferior longitudinal fasciculi. In a second investigation, we assessed the effect of white matter damage on processing speed using voxel-based lesion symptom mapping (VLSM) analysis of data from seventy-two patients with left hemisphere strokes. Lesions in left parietal white matter, together with cortical lesions in supramarginal and angular gyri were associated with impaired performance. These findings suggest that cognitive processing speed, as assessed by the Digit-Symbol test, is closely related to the structural integrity of white matter tracts associated with parietal and temporal cortices and left middle frontal gyrus. Further, fiber tractography applied to VBM results and the patient findings suggest that the superior longitudinal fasciculus, a major tract subserving fronto-parietal integration, makes a prominent contribution to processing speed.

Keywords

Cognitive processing speed; diffusion tensor imaging; individual differences; magnetic resonance imaging; neural pathways; neuropsychology

²now at Research Service, Veterans Affairs Northern California Health Care System, Martinez, CA 94553

³now at Department of Brain and Cognitive Sciences, Massachusetts Institute of Technology, Cambridge, MA 02139

Publisher's Disclaimer: This is a PDF file of an unedited manuscript that has been accepted for publication. As a service to our customers we are providing this early version of the manuscript. The manuscript will undergo copyediting, typesetting, and review of the resulting proof before it is published in its final citable form. Please note that during the production process errors may be discovered which could affect the content, and all legal disclaimers that apply to the journal pertain.

INTRODUCTION

Performance on complex cognitive tasks depends on coordinated activity in distributed brain networks. The speed and efficiency with which information can be registered and integrated across multiple channels is an important factor in how well basic cognitive mechanisms can be recruited in the service of goal-oriented actions. Indeed, processing speed has been proposed to be a key cognitive resource, alongside with attention, working memory and inhibition, underlying performance in a wide range of cognitive domains (Kail and Salthouse, 1994). Accordingly, psychometric measures of processing speed correlate with performance in a broad range of cognitive domains (Kail and Salthouse, 1994; Li et al., 2004; Salthouse, 2005; Wechsler, 1997a), as well as age-related changes in cognition during the course of child development (Kail, 1991) and healthy aging (Salthouse, 1996).

White matter pathways of the brain mediate the long-range transmission of information across distributed brain networks, and support the synchronization and integration of operations carried out by individual brain areas (Mesulam, 2000; Mesulam, 1998). Major white matter tracts of the primate brain follow a basic architectural plan along which information flow across major brain regions is regulated (Felleman and Van Essen, 1991; Schmahmann and Pandya, 2006). Theoretical analyses of brain connectivity patterns indicate that distributed patterns of cortical activity can be accounted for to a large extent by the patterns of interaction afforded by the white matter fiber systems (Hilgetag et al., 2000; Kotter and Sommer, 2000). Individual differences in cognitive processing speed are likely to depend to a large extent on structural variations in the organization of these pathways, which both constrain and facilitate the communication and coordination among cortical nodes of brain-wide networks.

The speed with which neural signals are conducted across long myelinated axons in the central nervous system is related to their thickness and degree of myelination (Gutierrez et al., 1995; Tolhurst and Lewis, 1992; Waxman, 1980). Efficient communication and coordination across neural networks rely upon the temporal precision of neural signals (Engel et al., 2001), which in turn hinges on the structural properties of the fiber bundles serving neural signal transmission. Long distance transmission of signals across the cerebrum depends upon the ability of long association tracts to reduce signal degradation (Catani and ffytche, 2005). White matter diseases, such as multiple sclerosis which leads to demyelination, and wide spread damage across fiber systems, as occurs in traumatic brain injury, cause an overall slowing of cognitive processes (Levine et al., 2006; Rao, 1996).

Long association tracts subserve functional integration among frontal, parietal and temporal association cortices (Schmahmann and Pandya, 2006). The most prominent association tracts bridging frontal, temporal and parietal regions are the superior longitudinal fasciculus, inferior longitudinal fasciculus, occipito-frontal fasciculus, and the uncinate fasciculus. Higher-order association areas in prefrontal cortex and temporal and posterior parietal lobes are considered to have important roles in attention, working memory and response selection (Goldman-Rakic, 1988; Mesulam, 2000). These are the brain regions that are most commonly recruited by the diverse range of cognitive tasks used in neuroimaging studies (Cabeza and Nyberg, 2000; Duncan and Owen, 2000; Shulman et al., 1997). Functional coupling between posterior and frontal brain regions, mediated by long-range cortico-cortical association tracts, are construed as being central for carrying out mental operations (Goldman-Rakic 1998, Fuster, 2001).

We set out to test the hypothesis that structural features of major white matter fiber systems responsible for fronto-parietal and fronto-temporal interactions, as assessed by the fractional anisotropy measure, should be related to interindividual variations in cognitive processing speed, as assessed by the Digit-Symbol test, a standardized test of processing speed. In a second investigation, we assessed the effect of neurological damage due to stroke on Digit-Symbol

performance. We predicted that lesions affecting fronto-posterior association tracts should be associated with more severely impaired performance than lesions elsewhere.

In order to investigate the relationship between cognitive speed of processing and white matter organization, we first examined the relation between performance on the Digit-Symbol test and diffusion tensor imaging (DTI) of white matter, a technique which makes possible *in vivo* exploration of microstructural features of white matter with quantitative methods (Basser and Pierpaoli, 1996; Beaulieu, 2002; Le Bihan and van Zijl, 2002). The most commonly-used DTI-derived measure of white matter microstructure is fractional anisotropy (FA), a scalar quantity derived from diffusion tensors that reflects the degree to which diffusion of water molecules is constrained in space due to local tissue properties including density, directional coherence, diameter, and myelination level of white matter fibers (Basser and Pierpaoli, 1996), the same properties that influence neural signal transmission. The sensitivity of FA to local organization of fibers has been utilized to demonstrate correlations between psychological variables and subtle variations in regional properties of white matter structures that are not accessible through other imaging modalities (Deutsch et al., 2005; Klingberg et al., 2000; Madden et al., 2004; Moseley et al., 2002; Schulte et al., 2005; Tuch et al., 2005).

The Digit-Symbol subtest from the WAIS-III (Wechsler, 1997b) is a widely-used and standardized psychometric test that targets the ability to perform a series of elementary perceptual, cognitive, and motor operations fluently under time pressure. The Digit-Symbol test taps into an array of elementary cognitive processes including visual analysis, maintenance of stimulus-response associations, focused attention, response selection, and motor execution, and has high re-test reliability (Lezak, 1995; Salthouse, 2005; Wechsler, 1997b). Digit-Symbol performance is sensitive to white matter damage due to injury or disease (Charlton et al., 2006; O'Brien et al., 2002) and aging (Salthouse, 1996). Because of its psychometric properties, the Digit-Symbol test was adopted as the measure of processing speed for this investigation.

Voxel-based morphometry (Ashburner and Friston, 2000) was used to investigate the relationship between processing speed and regional microstructural organization of white matter, as indexed by fractional anisotropy, in healthy young subjects. Fiber tractography (Basser et al., 2000; Conturo et al., 1999; Mori and van Zijl, 2002) was utilized to identify the tracts most likely to be associated with the white matter regions determined by voxel-based morphometry.

The relation between processing speed and the integrity of white matter pathways was further investigated in a large group of neurological patients with left-hemisphere lesions due to stroke. Damage to brain regions subserving critical computations and the disruption of the white matter pathways that are essential for interregional interactions should have a negative impact on processing speed. Voxel-based lesion symptom mapping (VLSM), a statistical technique for quantitative assessment of the relation between damage to brain regions and continuous behavioral measures (Baldo and Dronkers, 2006; Bates et al., 2003; Dronkers et al., 2004), was employed. It was predicted that the findings from the two investigations, one with healthy subjects and the other with neurological patients would converge on the white matter regions critical for processing speed.

MATERIALS AND METHODS

Diffusion Tensor Imaging

Subjects—Thirty-nine right-handed healthy young adults (16 F, mean age=22.4±3, range=18–31), with no history of neurological or major psychiatric conditions by self-report, participated in the study. All participants signed a written informed consent form approved by the institutional review board of Stanford University.

Behavioral testing—The Digit-Symbol subtest from the Wechsler Adult Intelligence Scale-III (Wechsler, 1997b) was administered to assess processing speed. Subjects were presented with a key that associated the digits 1 to 9 with distinct symbols. They were asked to go through a list of digits arranged in rows on a paper sheet, and copy the corresponding symbol underneath each digit with a pencil. The number of digit-symbol pairs that were correctly completed under a two-minute time limit served as the measure of speed of processing. The mean raw Digit-Symbol score was 89.41 items (s.d. = 12.64, range 64–119), and the mean age-scaled score was 11.92 (s.d. = 2.36). There was a trend ($p = 0.073$) towards better Digit-Symbol performance for the women (mean = 93.75 items, s.d. = 10.45, range 80–119) compared to the men (86.39 items, s.d. = 13.36, range 64–118). Mean age did not differ ($p = 0.53$) between men (22.7, s.d. = 3.28) and women (22.06, s.d. = 2.77). Subjects also completed a test of general reasoning ability, Raven's Advanced Progressive Matrices Test (RAPM) (The Psychological Corporation, 1991), under a 40-minute time limit. Mean RAPM score was 28.63 (s.d. = 3.86, range 23–36). RAPM performance was used as a covariate to control for general ability differences.

DTI image acquisition—Magnetic resonance images were acquired on a GE-Signa 3-T scanner (General Electric, Milwaukee, Wisconsin) with a quadrature head coil. DT data were acquired using a single-shot echoplanar imaging sequence. The scanning parameters were: 128×128 imaging matrix, FOV=24×24 cm, TR/TE = 11600/64.5 ms. A total of 26 axial slices (4 mm thick, 1 mm interslice gap), covering the entire cerebrum and superior portion of the cerebellum, were acquired parallel to the bicommissural (AC-PC) axis. In each of six repeated acquisition cycles, one non-diffusion weighted ($b=0$) and 12 diffusion weighted ($b=800$ s/mm²) images were collected along 6 independent directions with reversal of gradient direction on alternating scans according to the following encoding scheme: $+x+y$, $-x-y$, $+y+z$, $-y-z$, $+x+z$, $-x-z$, $-x+y$, $x-y$, $-y+z$, $y-z$, $x-z$, $-x+z$. Reversal of gradient direction for alternating diffusion weighted images served to reduce cross terms from background gradients. A T2-weighted anatomic image (TR/TE = 3000/68 ms, FOV = 24cm, 256×256 matrix, 26 axial slices) in the same space as the DT images, and a T1-weighted high-resolution anatomic image (spoiled gradient recalled 3D MRI protocol, 124 sagittal slices, FOV = 24 cm, TR/TE = 24/5 ms, 256×256 matrix, 124 sagittal slices) were also acquired.

Postprocessing of DTI images—Diffusion weighted images were visually scanned in order to exclude slices with artifacts. In order to correct for eddy current-induced distortions and motion artifacts, all images with the same diffusion weighting and gradient direction were first realigned using a rigid body transformation. All images were then coregistered to the mean non-diffusion weighted (B0) image using a 12 parameter affine transformation and normalized mutual information coregistration. Tensor components and fractional anisotropy maps (Basser and Pierpaoli, 1996) were computed using the Diffusion Toolbox (<http://sourceforge.net/projects/spmtools>) for SPM5 (<http://www.fil.ion.ucl.ac.uk/spm>) implemented in Matlab (Mathworks, Natick, MA, USA).

The T1-weighted anatomical scan was realigned with the T2-weighted anatomic image acquired in the same space as the DT images using rigid body alignment. The voxel-based morphometry module of SPM5, which takes into account gray matter (GM), white matter (WM) and cerebrospinal fluid (CSF) components individually, was used to normalize the anatomical scan to standard (MNI) and to estimate intracranial volume. In order to correct for susceptibility induced distortions, the mean B0 image was coregistered to the T1-weighted anatomical scan using the nonlinear registration implemented in SPM5 VBM module, and the GM, WM and CSF segments obtained from the anatomical scan as tissue priors. The deformation fields resulting from the two transformations (T1 to MNI and B0 to T1) were combined and applied to the FA images, using tri-linear interpolation and a final spatial resolution of $2 \times 2 \times 2$ mm³. This procedure served to minimize interpolation errors, apply a

spatial transformation only to FA images which encode a rotation-invariant quantity, and ensure proper alignment of white matter, cortical and subcortical gray matter, and the ventricles across subjects.

White matter masks derived from T1-weighted anatomical images were applied to the normalized FA images, which were then smoothed with a 6mm FWHM Gaussian spatial filter. The 6-mm smoothing kernel was chosen to emphasize only thick bundles with diameters on the order of 0.6 cm, which is true of major tract systems (Makris et al., 1997).

Voxel-based Morphometry analysis (VBM)—The linear correlation between FA and Digit-Symbol performance (raw scores) was tested at each voxel with the multiple linear regression model implemented in SPM5. Age, sex and estimated total intracranial volume were included as covariates in the model. The resulting statistical parametric maps were thresholded at a significance level of $p < 0.005$ for each voxel, and an extent threshold of 50 contiguous voxels (0.4 ml.) for each cluster. Thresholded t-maps were overlaid on the average of normalized FA images from the whole group for visualization.

Fiber tractography—In order to perform fiber tractography on group data in standard space (Jones et al., 2002), a generic set of tensor components were derived by applying tensor regression to normalized diffusion-weighted images pooled across all subjects. Images were averaged across repetitions prior to normalization, and gradient vectors were reoriented to adjust for the rotational component of the normalization transformation (Alexander et al., 2001). The primary orientation of the principal diffusion direction for each volume of interest was determined from the group map. Fiber tracking was performed using the streamline tracking with 4th order Runge-Kutta integration method (step size = 1 mm, minimum length = 10 mm, stopping criterion: FA = 0.2, angle = 75°) implemented in DoDTI software (<http://neuroimage.yonsei.ac.kr/dodti>) (Park et al., 2004). Seed points for tractography were determined by the regions of interest derived from VBM results.

Fiber tract identification—White matter labels from the Talairach and Tournoux atlas (Talairach, 1988), a published white matter tractography atlas (Wakana et al., 2004), a detailed investigation of major fiber tract trajectories using human postmortem brains (Burgel et al., 2006) and a primate brain white matter atlas (Schmahmann and Pandya, 2006), were consulted in order to identify the candidate fiber tracts associated with the regions where the correlations were found in VBM analysis of the DTI data.

Voxel-based Lesion-Symptom Mapping (VLSM)

Neurological patients—A group of 72 left-hemisphere stroke patients (18 F, all pre-morbidly right-handed, mean age 61.1 ± 11.6 years, range 31–80, all with a single cerebrovascular accident) were tested in the chronic phase of their injury (at least 12 months post-onset). Before testing, participants read and signed consent forms approved by the Institutional Review Board of the VA Northern California Health Care System, Martinez, CA and in accordance with the Helsinki Declaration (World Medical Association, 2004).

Behavioral testing—The Digit-Symbol subtest from the Wechsler Adult Intelligence Scale-III (Wechsler, 1997b) was administered as part of a larger battery at the Center for Aphasia and Related Disorders, VA Northern California Health Care System (VANCHCS), Martinez, CA. Patients who had a right-sided weakness used their left hands. The mean raw score was 26.97 items (s.d. = 13.94), and the mean age-scaled score was 4.5 (s.d. = 1.92). The average performance of the patient group was below the expected level for the normal population.

Voxel-based Lesion-Symptom Mapping analysis—Patients' lesions, imaged at least three weeks post-stroke, were reconstructed onto standardized brain templates by a board-certified neurologist, transcribed to MNI space, and stored in image volumes with $2 \times 2 \times 2$ mm voxel resolution. For a majority of patients, MRI scans were used. Computed tomography images were used in cases where MRI scans were not available. Lesion data (binary images in which the value at each voxel indicates the absence or presence of a lesion) and behavioral scores (Digit-Symbol raw scores adjusted for age and gender) for each patient were entered into VLSM analysis (Bates et al., 2003) (<http://crl.ucsd.edu/vlsm>). At each voxel, a t-test compared the performance levels of patients with and without a lesion at that voxel. A voxel was included in the analysis only if at least 10 patients had a lesion at that location. The resulting t-map was thresholded at a significance level of $p < 0.005$. The mean normalized FA map for the subjects in the first investigation was used to visualize the extent of the white matter lesions associated with impaired performance.

RESULTS

Diffusion Tensor Imaging

After correcting for age, gender and intracranial volume, regions of cerebral white matter containing voxels where fractional anisotropy was correlated positively with processing speed were clustered in five groups (Table 1, Figure 1–Figure 2). These clusters lay in parietal lobes bilaterally, left superior frontal lobe (middle frontal gyrus), and bilateral temporal lobes. No negative correlations were found, even at the reduced threshold of $p < 0.01$; extent > 25 voxels. Neither were any correlations found between regional gray matter density and processing speed, as assessed by VBM analysis of T1-weighted anatomical scans.

The dominant primary eigenvector direction in the temporal-lobe volumes of interest was anterior-posterior (left - 77/77, right - 87/129 voxels) (Figure 2). The parietal ROIs had voxels with anterior-posterior (left 47/74, right, 64/95) and superior-inferior (left - 27/74, right - 31/95) orientations. The majority of fibers in left frontal ROI had medial-lateral (23/57) and anterior-posterior (20/57) orientations. Stepwise regression (Matlab Statistics toolbox) was used to determine the regions contributing most to the variance in Digit-Symbol scores, after partialing out age and sex. A model including only the mean FA values for left parietal and right temporal white matter regions (Figure 3) accounted for the largest amount of variance in Digit-Symbol scores adjusted for age and sex (adjusted multiple $R^2 = 0.62$, $F(2,36)=33.79$, $p < 0.001$). The relation between Digit-Symbol performance and FA values in these regions remained significant when general reasoning ability, as assessed by the Raven's Progressive Matrices test, was used as a covariate.

Fiber tractography results suggested that the bilateral temporal regions of interest are consistent with inferior longitudinal fasciculus and inferior occipito-frontal fasciculus, and the parietal regions of interest with the superior longitudinal fasciculus and posterior section of the corona radiata (Figure 4). The left superior frontal white matter lies on a tract with both an anterior-posterior and superior-inferior orientation. Tractography defined fibers terminate in close proximity to the extreme capsule and left putamen, consistent both with fronto-striatal projections and the fibers through the extreme capsule that connect lateral prefrontal cortex with middle and inferior temporal regions.

The primary goal of this investigation was to study white matter microstructure in relation to processing speed independently of possible sex differences. Since there is recent evidence for sex differences in brain morphology related to intellectual functioning (Haier et al., 2005a; Narr et al., 2006), a subsidiary analysis was carried out modeling the Digit-Symbol scores of male and female subjects with separate covariates in the design matrix. Age and intracranial volumes for both groups were used as extraneous variables. The same statistical thresholds as

in the main analysis ($p < 0.005$ and extent > 50 voxels) were used. For females, FA was positively correlated with Digit-Symbol performance only in bilateral temporal and left parietal white matter. For males, in addition to the bilateral parietal, temporal and left frontal white matter regions, an additional cluster in the anterior portion of the corpus callosum showed a significant positive correlation (peak coordinates = 0 20 18 mm, cluster size = 61 voxels).

Voxel-based Lesion-Symptom Mapping investigation

VLSM analysis revealed an association between deficits in processing speed and lesions in parietal white matter, including the superior longitudinal fasciculus and the corona radiata (Figures 5A, B). Other white matter foci were in the pyramidal tract, the external capsule, and the anterior and posterior limbs of the internal capsule. Gray matter lesions affecting processing speed were found in parietal association cortex (Brodmann's areas 39 and 40), postcentral gyrus, Heschl's gyrus and caudate nucleus and the putamen. However, the unique contribution of white matter damage to impaired performance could not be established, since the distribution of the lesions did not allow investigation of the effects of isolated parietal white matter or gray matter damage. The VBM-derived region of significant association from the first investigation and the VLSM regions of significance overlapped in left parietal white matter, and this region of overlap was consistent with the trajectory of the superior longitudinal fasciculus (Figure 6, 7).

DISCUSSION

Cognitive processing speed, as assessed by the Digit-Symbol Substitution subtest from WAIS-III, correlated positively with regional FA values in white matter of the left middle frontal gyrus, bilateral parietal lobes, and bilateral temporal lobes in a group of young healthy adults. Left parietal and right temporal regions were most strongly associated with inter-individual variance in processing speed. The anatomical locations of the regions of correlation are consistent with the trajectories of major white matter tracts running along the anterior-posterior axis of the brain that support fronto-posterior network interactions. Fiber tracking applied to the group tensor map suggests that these tracts are the superior longitudinal fasciculus, occipito-frontal fasciculus, inferior longitudinal fasciculus, as well as the posterior corona radiata. A second investigation using voxel-based lesion-symptom mapping analysis of neurological patient data indicated that left parietal lobe lesions extending deeply into white matter are associated with poorer Digit-Symbol performance than lesions elsewhere.

Role of long white matter association tracts in processing speed

The results of the DTI investigation support the idea that parietal white matter plays an important role in cognitive processing speed (Figure 7). Fractional anisotropy in left parietal white matter had the strongest relation to cognitive processing speed in the DTI analysis (adjusted $R^2 = 0.52$). The tractography results indicate that this region of significant association is consistent with the trajectory of the superior longitudinal fasciculus (Burgel et al., 2006; Mori et al., 2002; Schmahmann and Pandya, 2006), which projects to superior frontal cortex and temporal regions. Neurological patients with lesions in left parietal white matter, encompassing the region found in the DTI investigation, and neighboring cortical regions BA 39 and 40 were found to have reduced processing speed compared to patients who did not have lesions in these areas.

Based on an extensive review of the literature on the relation between intelligence and brain function, it has recently been proposed that the connections between frontal and parietal areas play an important role in general intellectual ability (Jung and Haier, 2007). The reciprocal projections between posterior parietal and dorsolateral prefrontal cortices (Goldman-Rakic, 1988; Schmahmann and Pandya, 2006) form part of the SLF complex (Makris et al., 2005)

and subserve action sequences extending across time (Fuster, 2004). Fractional anisotropy in left frontal and inferior parietal white matter, consistent with the trajectory of the superior longitudinal fasciculus, has recently been reported to be associated with faster performance on a lexical decision task (Gold et al., 2007). Another recent investigation has found a relation between physiological measures of functional connectivity during performance in a choice reaction time task and FA values in the white matter pathways interconnecting cortical regions that mediate action selection, including the superior longitudinal fasciculus (Boorman et al., 2007).

The neurological patient findings in this investigation suggest that cortical areas BA 39 and 40 and the underlying intracortical white matter play a critical role in the neural computations underlying Digit-Symbol performance. Parietal areas BA 39, 40 and 7 are active in virtually all neuroimaging studies of high-level cognition (Cabeza and Nyberg, 2000). Posterior parietal lesions extending into white matter affect perceptual processing speed (Peers et al., 2005). White matter volume and metabolic activity in posterior parietal lobe correlate with general intellectual ability assessed with the WAIS-III (Haier et al., 2004). A functional brain imaging investigation found that better performance on the Digit-Symbol test is associated with higher BA 40 activity (Rypma et al., 2006). Consistent with a role in representing a repertoire of response alternatives (Bunge et al., 2002), areas BA 39 and BA 40 might be necessary for establishing and maintaining the associations between digits and symbols, which in turn are selected through frontal lobe control mechanisms (Bunge et al., 2002; Gabrieli et al., 1998). The interplay between left frontal and posterior association areas, mediated by the SLF, might be critical for maintaining a task set that ensures fluid execution of the sequence of operations taxed by the Digit-Symbol test.

Fiber tractography results suggest that the frontal region of significance in this investigation might lie along fronto-striatal projections, though it does not preclude the involvement of other tracts. Dorsolateral prefrontal cortex, a key nodal point the networks that subserve cognition (Cabeza and Nyberg, 2000; Duncan and Owen, 2000; Shulman et al., 1997), is connected with (1) posterior parietal and occipital areas through the superior fronto-occipital fasciculus (SOF); (2) dorsomedial thalamic nuclei through anterior thalamic projections; (3) prefrontal cortex of the contralateral hemisphere through transcallosal fiber tracts; and (4) the basal ganglia through fronto-striatal projections (Alexander et al., 1990; Burgel et al., 2006; Lehericy et al., 2004; Mori et al., 2002; Petrides, 2002; Schmahmann and Pandya, 2006). Consistent with the possible involvement of fronto-striatal projections, disruption of the loops through the basal ganglia due to pallidotomy reduces processing speed as assessed by the Digit-Symbol test (Stebbins et al., 2000).

The temporal-lobe white matter regions associated with processing speed encompass the inferior longitudinal fasciculus and the inferior occipito-frontal fasciculus that interconnect with the descending part of the superior longitudinal fasciculus and form a pathway that connects visual areas to the rest of the brain (Catani et al., 2003). The surrounding gray matter supports analysis of objects and their features (Cabeza and Nyberg, 2000). The left temporal region of significance extends anteriorly into the expected location of uncinate fasciculus (Burgel et al., 2006), the integrity of which is critical for learning associations between visual stimuli (Eacott and Gaffan, 1992). The right temporal region extends posteriorly into the territory of the optic radiation (Burgel et al., 2006). It can be presumed that these pathways are critical for relaying the analysis of visual features to centers involved in control of visual scanning and response selection, and their level of organization contributes to better performance on the Digit-Symbol test.

Based on the current findings, we hypothesize that the white matter FA correlations reported here reflect the functional neuroanatomy of long-range white matter fiber tracts that mediate

interactions between posterior association cortices for perceptual representations and visuo-spatial transformation, and the frontal lobe structures involved in attentional control and regulation of actions. Further investigations combining DTI with functional neuroimaging, as well as investigations of neurological patients with focal white matter lesions, will be useful for exploring this hypothesis.

Comparison of findings from the Diffusion Tensor Imaging and the Voxel-based Lesion-Symptom Mapping investigations

The findings from the diffusion tensor imaging investigation with healthy subjects are inherently correlational. The results from the neurological patients, on the other hand, suggest that the integrity of the left posterior parietal lobe and its white matter is necessary for efficient processing speed. The lesion-symptom mapping analysis, however, has certain limitations. Only left hemisphere lesions have been included in the analysis because most of the available scans came from patients with left-lateralized lesions. Some temporal lobe patients with severe Wernicke's aphasia could not be included because their comprehension deficits prevented test administration. The age-scaled performance level of the neurological patients is below the population average, and working memory and attention problems can contribute to poor performance at their performance level and age group. Some patients had to use their non-dominant hands, possibly slowing their performance. Further, and more importantly, the respective contributions of parietal white matter and gray matter damage have not been established in this investigation, and require testing patients with focal white matter injury. However, the findings from the two independent investigations both point to major left parietal white matter involvement in processing speed.

Processing speed and brain networks

We investigated perceptual-motor processing speed because it is viewed as an overall measure of cognitive mechanisms that are widely used to support fluent execution of perceptual, cognitive and motor processes (Lezak, 1995). Some studies have examined neural correlates of visual-choice reaction time as a similar measure of a core cognitive capacity. Visual choice reaction time in young healthy adults has been found to correlate with regional FA in a number of posterior regions, mainly in the right hemisphere (optic radiation, thalamus and precuneus) (Tuch et al., 2005). Another study reported an association between simple reaction time and white matter density in right fusiform gyrus using T1-weighted structural images (Haier et al., 2005b). We found a broader involvement of left frontal, parietal and temporal regions, possibly because of the broader cognitive demands of the Digit Symbol task. The temporal and parietal regions of the right hemisphere specialize in receptive aspects of visuo-spatial processing (Corbetta and Shulman, 2002). On the other hand, the production of actions is associated with a left fronto-parietal network, the disruption of which leads to apraxias (Catani and ffytche, 2005). Lesions to left dorsolateral prefrontal cortex make response times in cognitive tasks slower and more variable (Stuss et al., 2003). Left frontal areas also play a role in the selection of responses from a repertoire of alternatives (Gabrieli et al., 1998), which are likely to be represented in left posterior regions (Bunge et al., 2002).

Two reports using region-of-interest based analyses of fractional anisotropy in large parcels of white matter have reported that total FA values in the splenial part of the corpus callosum correlate with finger-tapping rate in old adults (Sullivan et al., 2001) and choice reaction times in an oddball task in both young and old adults (Madden et al., 2004). Although we did not find an effect in the splenium, the tasks, age groups, and analysis methods used in these studies are not directly comparable. Future investigations using a wider range of cognitive tasks and analysis methods will be needed for a precise delineation of the fiber systems that become critical under different performance conditions and for different populations.

A preliminary exploration of possible sex differences in the relation between white matter microstructure and processing speed raises the possibility that performance differences among males might depend more strongly on white matter organization for males than females, and that male performance might rely more on left frontal white matter and the anterior corpus callosum. However, there are only 16 female and 23 male subjects. Females tended to be better performers and showed less variance in their performance. The analysis protocol does not attempt to reduce the effects of anatomical variability between males and females by using sex specific templates, as was done by Haier et al. (2005). These factors are likely to reduce the power to detect and characterize sex differences in the way white matter properties and processing speed are related, which should be elucidated by future investigations.

We did not find a relation between processing speed assessed via Digit-Symbol performance and regional gray matter concentration. A correlation has been reported between right temporal-lobe gray matter concentration and Digit-symbol performance in a VBM investigation using T1-weighted images from 48 young subjects, but this analysis yielded a single cluster consisting only of 7 voxels (Colom et al., 2006). Another VBM study with 9 middle-aged and 8 old adults reported no positive correlations between regional gray matter concentration and reaction times (RT) in a visual stimulus-response task, and a negative correlation between gray matter concentration in globus pallidus, parahippocampus, and thalamus and RTs in a visual recognition memory task (Haier et al., 2005b). Interestingly, in some regions gray matter concentration was associated with faster RTs in middle-aged subjects but slower RTs for older subjects.

It is possible that the most significant factor limiting the processing power of complex cerebral circuits on a task that requires execution of multiple operations, such as the Digit-Symbol test, might be the capacity of white matter tracts to support efficient transmission of neural signals. Theoretically, at the cellular level, there must be many correlated properties between cell bodies (grey matter) and their myelinated axons (white matter), but different imaging measures vary in their sensitivity and limitations. DTI-derived measures of white matter organization may offer a more sensitive measure than VBM measures of gray matter concentration. High variability in gyral anatomy might reduce the sensitivity of gray matter VBM analysis, and larger subject groups with broader performance distributions might reveal gray matter involvement. Further developments in imaging technologies and image processing technique may provide better insight into the relative contributions of microstructural properties of gray and white matter to inter-individual differences.

Processing speed in each particular task is likely to depend to a large extent on the properties of the specific white matter fiber tracts responsible for transmitting the information and control signals that are essential for performance on that task. Consistent with its established role as a psychometric test and neuropsychological assessment tool, the Digit-Symbol test engages a broad range of cognitive, perceptual and motor processes, making it well-suited for highlighting the fiber systems that are commonly recruited by a variety of cognitive processes and their role on the speed and efficiency with which these processes are executed.

In conclusion, we have found evidence for which white matter pathways might be essential for processing speed, often viewed as a key primitive for the cognitive architecture (Kail and Salthouse, 1994). Voxel-based analysis of diffusion tensor images and fiber tractography findings indicated that variations in the microstructure of white matter tracts interconnecting brain region that subserves high-level cognition can account for variations in a psychometric measure of processing speed among healthy young adults. Assessment of the effects of brain lesions on performance on the same task provided results consistent with a critical role for left posterior parietal lobe and its white matter. The present findings motivate further research in

this area, and can inform investigations of cognitive development, the process of healthy aging, and cognitive impairments in clinical conditions that affect brain white matter.

ACKNOWLEDGEMENTS

This work was supported by grants from National Institutes of Health (MH61426 and 1 F32 NS43961), the Department of Veterans Affairs Division of Medicine and Surgery, National Institute for Neurological Disorders and Stroke (P01 NS17778, P01 NS40813) and the National Institute of Deafness and Communication Disorders (NIH/NIDCD 2 RO1 DC00216). We thank Yuki Yamaguchi for her assistance in data collection and analysis, and Dr. Katrin Amunts and Dr. Hartmut Mohlberg for providing the probabilistic map of the superior longitudinal fasciculus.

REFERENCES

- Alexander DC, Pierpaoli C, Basser PJ, Gee JC. Spatial transformations of diffusion tensor magnetic resonance images. *IEEE Trans Med Imaging* 2001;20:1131–1139. [PubMed: 11700739]
- Alexander GE, Crutcher MD, DeLong MR. Basal ganglia-thalamocortical circuits: parallel substrates for motor, oculomotor, "prefrontal" and "limbic" functions. *Prog Brain Res* 1990;85:119–146. [PubMed: 2094891]
- Ashburner J, Friston KJ. Voxel-based morphometry--the methods. *Neuroimage* 2000;11:805–821. [PubMed: 10860804]
- Baldo JV, Dronkers NF. Neural correlates of arithmetic and language comprehension: A common substrate? *Neuropsychologia*. 2006
- Basser PJ, Pajevic S, Pierpaoli C, Duda J, Aldroubi A. In vivo fiber tractography using DT-MRI data. *Magn Reson Med* 2000;44:625–632. [PubMed: 11025519]
- Basser PJ, Pierpaoli C. Microstructural and physiological features of tissues elucidated by quantitative-diffusion-tensor MRI. *J Magn Reson B* 1996;111:209–219. [PubMed: 8661285]
- Bates E, Wilson SM, Saygin AP, Dick F, Sereno MI, Knight RT, Dronkers NF. Voxel-based lesion-symptom mapping. *Nat Neurosci* 2003;6:448–450. [PubMed: 12704393]
- Beaulieu C. The basis of anisotropic water diffusion in the nervous system - a technical review. *NMR Biomed* 2002;15:435–455. [PubMed: 12489094]
- Boorman ED, O'Shea J, Sebastian C, Rushworth MF, Johansen-Berg H. Individual differences in white-matter microstructure reflect variation in functional connectivity during choice. *Curr Biol* 2007;17:1426–1431. [PubMed: 17689962]
- Bunge SA, Hazeltine E, Scanlon MD, Rosen AC, Gabrieli JD. Dissociable contributions of prefrontal and parietal cortices to response selection. *Neuroimage* 2002;17:1562–1571. [PubMed: 12414294]
- Burgel U, Amunts K, Hoemke L, Mohlberg H, Gilsbach JM, Zilles K. White matter fiber tracts of the human brain: three-dimensional mapping at microscopic resolution, topography and intersubject variability. *Neuroimage* 2006;29:1092–1105. [PubMed: 16236527]
- Cabeza R, Nyberg L. Imaging cognition II: An empirical review of 275 PET and fMRI studies. *J Cogn Neurosci* 2000;12:1–47. [PubMed: 10769304]
- Catani M, ffytche DH. The rises and falls of disconnection syndromes. *Brain* 2005;128:2224–2239. [PubMed: 16141282]
- Catani M, Jones DK, Donato R, Ffytche DH. Occipito-temporal connections in the human brain. *Brain* 2003;126:2093–2107. [PubMed: 12821517]
- Charlton RA, Barrick TR, McIntyre DJ, Shen Y, O'Sullivan M, Howe FA, Clark CA, Morris RG, Markus HS. White matter damage on diffusion tensor imaging correlates with age-related cognitive decline. *Neurology* 2006;66:217–222. [PubMed: 16434657]
- Colom R, Jung RE, Haier RJ. Distributed brain sites for the g-factor of intelligence. *Neuroimage* 2006;31:1359–1365. [PubMed: 16513370]
- Conturo TE, Lori NF, Cull TS, Akbudak E, Snyder AZ, Shimony JS, McKinstry RC, Burton H, Raichle ME. Tracking neuronal fiber pathways in the living human brain. *Proc Natl Acad Sci U S A* 1999;96:10422–10427. [PubMed: 10468624]
- Corbetta M, Shulman GL. Control of goal-directed and stimulus-driven attention in the brain. *Nat Rev Neurosci* 2002;3:201–215. [PubMed: 11994752]

- Deutsch GK, Dougherty RF, Bammer R, Siok WT, Gabrieli JD, Wandell B. Children's reading performance is correlated with white matter structure measured by diffusion tensor imaging. *Cortex* 2005;41:354–363. [PubMed: 15871600]
- Dronkers NF, Wilkins DP, Van Valin RD Jr, Redfern BB, Jaeger JJ. Lesion analysis of the brain areas involved in language comprehension. *Cognition* 2004;92:145–177. [PubMed: 15037129]
- Duncan J, Owen AM. Common regions of the human frontal lobe recruited by diverse cognitive demands. *Trends Neurosci* 2000;23:475–483. [PubMed: 11006464]
- Eacott MJ, Gaffan D. Inferotemporal-frontal Disconnection: The Uncinate Fascicle and Visual Associative Learning in Monkeys. *Eur J Neurosci* 1992;4:1320–1332. [PubMed: 12106395]
- Engel AK, Fries P, Singer W. Dynamic predictions: oscillations and synchrony in top-down processing. *Nat Rev Neurosci* 2001;2:704–716. [PubMed: 11584308]
- Felleman DJ, Van Essen DC. Distributed hierarchical processing in the primate cerebral cortex. *Cereb Cortex* 1991;1:1–47. [PubMed: 1822724]
- Fuster JM. Upper processing stages of the perception-action cycle. *Trends Cogn Sci* 2004;8:143–145. [PubMed: 15551481]
- Gabrieli JD, Poldrack RA, Desmond JE. The role of left prefrontal cortex in language and memory. *Proc Natl Acad Sci U S A* 1998;95:906–913. [PubMed: 9448258]
- Gold BT, Powell DK, Xuan L, Jiang Y, Hardy PA. Speed of lexical decision correlates with diffusion anisotropy in left parietal and frontal white matter: Evidence from diffusion tensor imaging. *Neuropsychologia*. 2007
- Goldman-Rakic PS. Topography of cognition: parallel distributed networks in primate association cortex. *Annu Rev Neurosci* 1988;11:137–156. [PubMed: 3284439]
- Gutierrez R, Boison D, Heinemann U, Stoffel W. Decompaction of CNS myelin leads to a reduction of the conduction velocity of action potentials in optic nerve. *Neurosci Lett* 1995;195:93–96. [PubMed: 7478276]
- Haier RJ, Jung RE, Yeo RA, Head K, Alkire MT. Structural brain variation and general intelligence. *Neuroimage* 2004;23:425–433. [PubMed: 15325390]
- Haier RJ, Jung RE, Yeo RA, Head K, Alkire MT. The neuroanatomy of general intelligence: sex matters. *Neuroimage* 2005a;25:320–327. [PubMed: 15734366]
- Haier RJ, Jung RE, Yeo RA, Head K, Alkire MT. Structural brain variation, age, and response time. *Cogn Affect Behav Neurosci* 2005b;5:246–251. [PubMed: 16180630]
- Hilgetag CC, Burns GA, O'Neill MA, Scannell JW, Young MP. Anatomical connectivity defines the organization of clusters of cortical areas in the macaque monkey and the cat. *Philos Trans R Soc Lond B Biol Sci* 2000;355:91–110. [PubMed: 10703046]
- Jones DK, Griffin LD, Alexander DC, Catani M, Horsfield MA, Howard R, Williams SC. Spatial normalization and averaging of diffusion tensor MRI data sets. *Neuroimage* 2002;17:592–617. [PubMed: 12377137]
- Jung RE, Haier RJ. The Parieto-Frontal Integration Theory (P-FIT) of Intelligence: Converging Neuroimaging Evidence. *Behavioral and Brain Sciences*. 2007(In Press)
- Kail R. Developmental change in speed of processing during childhood and adolescence. *Psychol Bull* 1991;109:490–501. [PubMed: 2062981]
- Kail R, Salthouse TA. Processing speed as a mental capacity. *Acta Psychol (Amst)* 1994;86:199–225. [PubMed: 7976467]
- Klingberg T, Hedehus M, Temple E, Salz T, Gabrieli JD, Moseley ME, Poldrack RA. Microstructure of temporo-parietal white matter as a basis for reading ability: evidence from diffusion tensor magnetic resonance imaging. *Neuron* 2000;25:493–500. [PubMed: 10719902]
- Kotter R, Sommer FT. Global relationship between anatomical connectivity and activity propagation in the cerebral cortex. *Philos Trans R Soc Lond B Biol Sci* 2000;355:127–134. [PubMed: 10703048]
- Le Bihan D, van Zijl P. From the diffusion coefficient to the diffusion tensor. *NMR Biomed* 2002;15:431–434. [PubMed: 12489093]
- Lehericy S, Ducros M, Van de Moortele PF, Francois C, Thivard L, Poupon C, Swindale N, Ugurbil K, Kim DS. Diffusion tensor fiber tracking shows distinct corticostriatal circuits in humans. *Ann Neurol* 2004;55:522–529. [PubMed: 15048891]

- Levine B, Fujiwara E, O'Connor C, Richard N, Kovacevic N, Mandic M, Restagno A, Easdon C, Robertson IH, Graham SJ, Cheung G, Gao F, Schwartz ML, Black SE. In vivo characterization of traumatic brain injury neuropathology with structural and functional neuroimaging. *J Neurotrauma* 2006;23:1396–1411. [PubMed: 17020478]
- Lezak, MD. Neuropsychological assessment. 3rd ed.. New York: Oxford University Press; 1995.
- Li SC, Lindenberger U, Hommel B, Aschersleben G, Prinz W, Baltes PB. Transformations in the couplings among intellectual abilities and constituent cognitive processes across the life span. *Psychol Sci* 2004;15:155–163. [PubMed: 15016286]
- Madden DJ, Whiting WL, Huettel SA, White LE, MacFall JR, Provenzale JM. Diffusion tensor imaging of adult age differences in cerebral white matter: relation to response time. *Neuroimage* 2004;21:1174–1181. [PubMed: 15006684]
- Makris N, Kennedy DN, McInerney S, Sorensen AG, Wang R, Caviness VS Jr, Pandya DN. Segmentation of subcomponents within the superior longitudinal fascicle in humans: a quantitative, in vivo, DT-MRI study. *Cereb Cortex* 2005;15:854–869. [PubMed: 15590909]
- Makris N, Worth AJ, Sorensen AG, Papadimitriou GM, Wu O, Reese TG, Wedeen VJ, Davis TL, Stakes JW, Caviness VS, Kaplan E, Rosen BR, Pandya DN, Kennedy DN. Morphometry of in vivo human white matter association pathways with diffusion-weighted magnetic resonance imaging. *Ann Neurol* 1997;42:951–962. [PubMed: 9403488]
- Mesulam M. Brain, mind, and the evolution of connectivity. *Brain Cogn* 2000;42:4–6. [PubMed: 10739582]
- Mesulam MM. From sensation to cognition. *Brain* 1998;121(Pt 6):1013–1052. [PubMed: 9648540]
- Mori S, Kaufmann WE, Davatzikos C, Stieltjes B, Amodei L, Fredericksen K, Pearlson GD, Melhem ER, Solaiyappan M, Raymond GV, Moser HW, van Zijl PC. Imaging cortical association tracts in the human brain using diffusion-tensorbased axonal tracking. *Magn Reson Med* 2002;47:215–223. [PubMed: 11810663]
- Mori S, van Zijl PC. Fiber tracking: principles and strategies - a technical review. *NMR Biomed* 2002;15:468–480. [PubMed: 12489096]
- Moseley M, Bammer R, Illes J. Diffusion-tensor imaging of cognitive performance. *Brain Cogn* 2002;50:396–413. [PubMed: 12480486]
- Narr KL, Woods RP, Thompson PM, Szeszko P, Robinson D, Dimtcheva T, Gurbani M, Toga AW, Bilder RM. Relationships between IQ and Regional Cortical Gray Matter Thickness in Healthy Adults. *Cereb Cortex*. 2006
- O'Brien JT, Wiseman R, Burton EJ, Barber B, Wesnes K, Saxby B, Ford GA. Cognitive associations of subcortical white matter lesions in older people. *Ann N Y Acad Sci* 2002;977:436–444. [PubMed: 12480784]
- Park HJ, Kubicki M, Westin CF, Talos IF, Brun A, Peiper S, Kikinis R, Jolesz FA, McCarley RW, Shenton ME. Method for combining information from white matter fiber tracking and gray matter parcellation. *AJNR Am J Neuroradiol* 2004;25:1318–1324. [PubMed: 15466325]
- Peers PV, Ludwig CJ, Rorden C, Cusack R, Bonfiglioli C, Bundesen C, Driver J, Antoun N, Duncan J. Attentional functions of parietal and frontal cortex. *Cereb Cortex* 2005;15:1469–1484. [PubMed: 15689522]
- Petrides, M.; Pandya, DN. Association Pathways of the Prefrontal Cortex and Functional Observations. In: Knight, DTSaRT., editor. *Principles of the Frontal lobe Function*. New York: Oxford University Press; 2002. p. 31-50.
- Rao SM. White matter disease and dementia. *Brain Cogn* 1996;31:250–268. [PubMed: 8812003]
- Rypma B, Berger JS, Prabhakaran V, Bly BM, Kimberg DY, Biswal BB, D'Esposito M. Neural correlates of cognitive efficiency. *Neuroimage* 2006;33:969–979. [PubMed: 17010646]
- Salthouse TA. The processing-speed theory of adult age differences in cognition. *Psychol Rev* 1996;103:403–428. [PubMed: 8759042]
- Salthouse TA. Relations between cognitive abilities and measures of executive functioning. *Neuropsychology* 2005;19:532–545. [PubMed: 16060828]
- Schmahmann, JD.; Pandya, DN. *Fiber pathways of the brain*. New York: Oxford University Press, Oxford; 2006.

- Schulte T, Sullivan EV, Muller-Oehring EM, Adalsteinsson E, Pfefferbaum A. Corpus callosal microstructural integrity influences interhemispheric processing: a diffusion tensor imaging study. *Cereb Cortex* 2005;15:1384–1392. [PubMed: 15635059]
- Shulman GL, Corbetta M, Buckner RL, Raichle ME, Fiez JA, Miezin FM, Petersen SE. Top-down modulation of early sensory cortex. *Cereb Cortex* 1997;7:193–206. [PubMed: 9143441]
- Stebbins GT, Gabrieli JD, Shannon KM, Penn RD, Goetz CG. Impaired frontostriatal cognitive functioning following posteroventral pallidotomy in advanced Parkinson's disease. *Brain Cogn* 2000;42:348–363. [PubMed: 10753484]
- Stuss DT, Murphy KJ, Binns MA, Alexander MP. Staying on the job: the frontal lobes control individual performance variability. *Brain* 2003;126:2363–2380. [PubMed: 12876148]
- Sullivan EV, Adalsteinsson E, Hedehus M, Ju C, Moseley M, Lim KO, Pfefferbaum A. Equivalent disruption of regional white matter microstructure in ageing healthy men and women. *Neuroreport* 2001;12:99–104. [PubMed: 11201100]
- Talairach, J.; Tournoux, P. Co-Planar Stereotaxic Atlas of the Human Brain. New York: Thieme; 1988.
- The Psychological Corporation. Raven Advanced Progressive Matrices. 1991
- Tolhurst DJ, Lewis PR. Effect of myelination on the conduction velocity of optic nerve fibres. *Ophthalmic Physiol Opt* 1992;12:241–243. [PubMed: 1408181]
- Tuch DS, Salat DH, Wisco JJ, Zaleta AK, Hevelone ND, Rosas HD. Choice reaction time performance correlates with diffusion anisotropy in white matter pathways supporting visuospatial attention. *Proc Natl Acad Sci U S A* 2005;102:12212–12217. [PubMed: 16103359]
- Wakana S, Jiang H, Nagae-Poetscher LM, van Zijl PC, Mori S. Fiber tract-based atlas of human white matter anatomy. *Radiology* 2004;230:77–87. [PubMed: 14645885]
- Waxman SG. Determinants of conduction velocity in myelinated nerve fibers. *Muscle Nerve* 1980;3:141–150. [PubMed: 6245357]
- Wechsler, D. WAIS-III WMS-III TECHNICAL MANUAL. San Antonio, TX: The Psychological Corporation; 1997a.
- Wechsler, D. Wechsler Adult Intelligence Scale-III. San Antonio, TX: The Psychological Corporation; 1997b.
- World Medical Association. Declaration of Helsinki: ethical principles for medical research involving human subjects. *J Int Bioethique* 2004;15:124–129. [PubMed: 15835069]

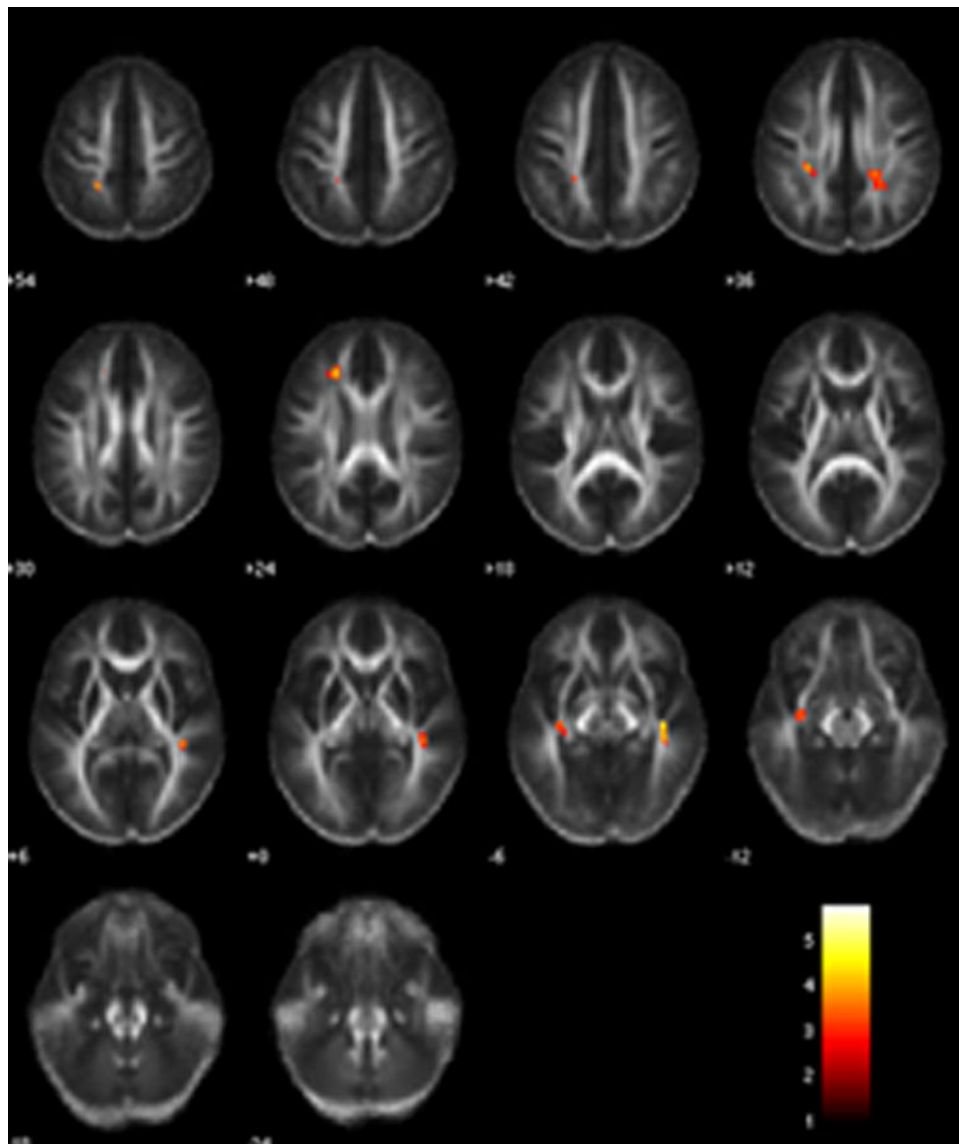


Figure 1. White matter regions showing a positive correlation between FA and processing speed. Axial cross sections, overlaid on the average normalized FA image for the group, run along the superior to inferior direction in steps of 6 mm ($z = 54$ mm to -24 mm). Parietal regions of significance are shown at the top row, left frontal region in second row, and temporal regions at the third row. Colorbar indicates the t-values for the regression slopes. In this and the following figures the neurological convention is followed (left side of the brain is shown on the left side of the figure).

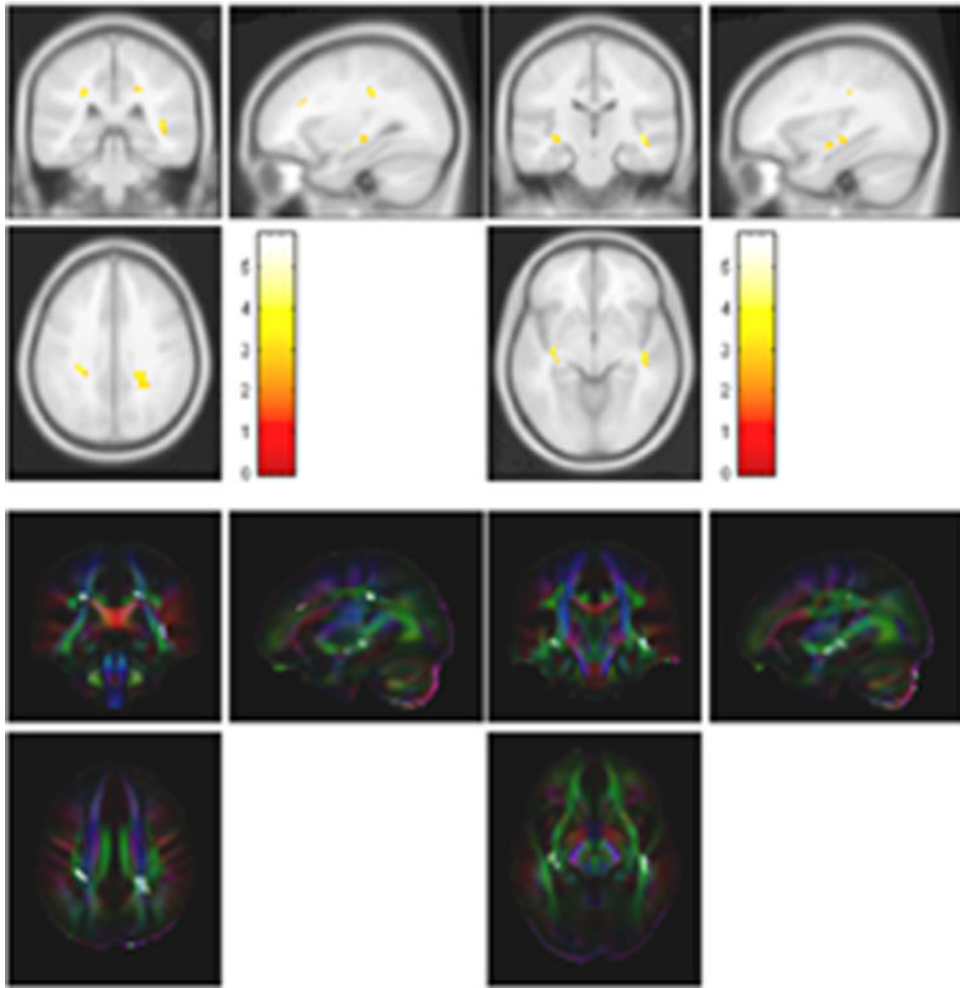


Figure 2.

Orthogonal views of the white matter regions showing positive correlation between fractional anisotropy and processing speed superimposed on the Montreal Neurological Institute T1-weighted brain template (top row) and color coded primary eigenvector maps (bottom row, red = medio-lateral, blue = superior-inferior, green = anterior-posterior directions). Parietal and frontal regions of significant association can be seen in the left column, and temporal regions in the right. Their relation to major brain landmarks and white matter tracts can be appreciated. Cross-sections were taken at $x = -30, y = -35, z = 35$ mm (left column) and $x = -33, y = -22, z = 4$ mm (right column).

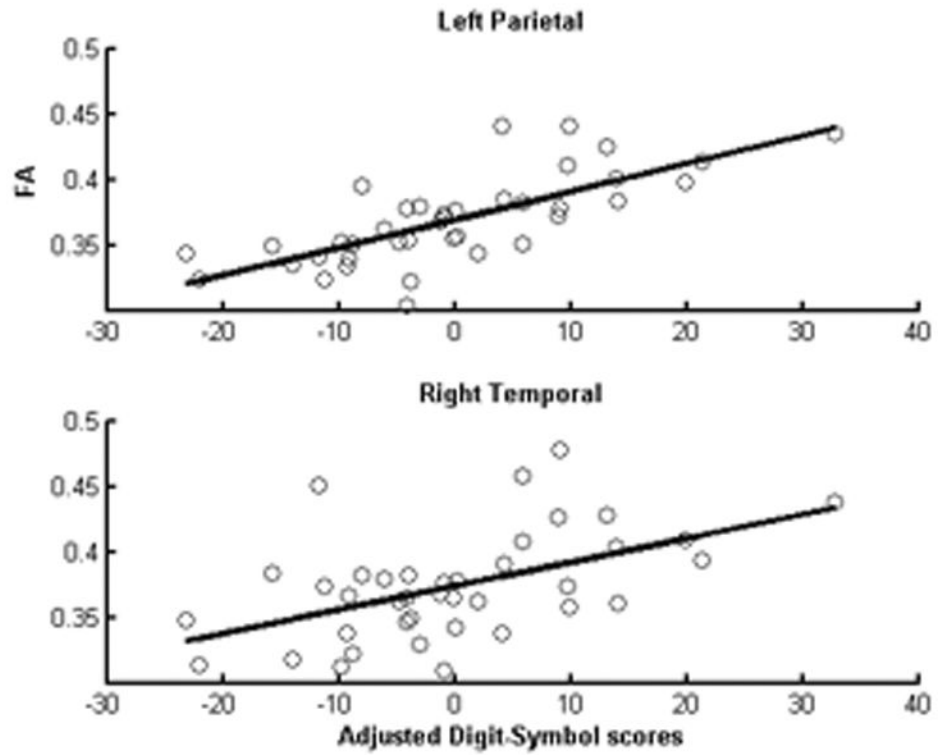


Figure 3. Scatter plots showing mean fractional anisotropy for left superior parietal and right temporal white matter against the distribution of Digit-Symbol scores adjusted for age and sex. FA values were extracted from the unsmoothed normalized FA maps using the regions of significance from the VBM analysis and masked to exclude non-white matter.

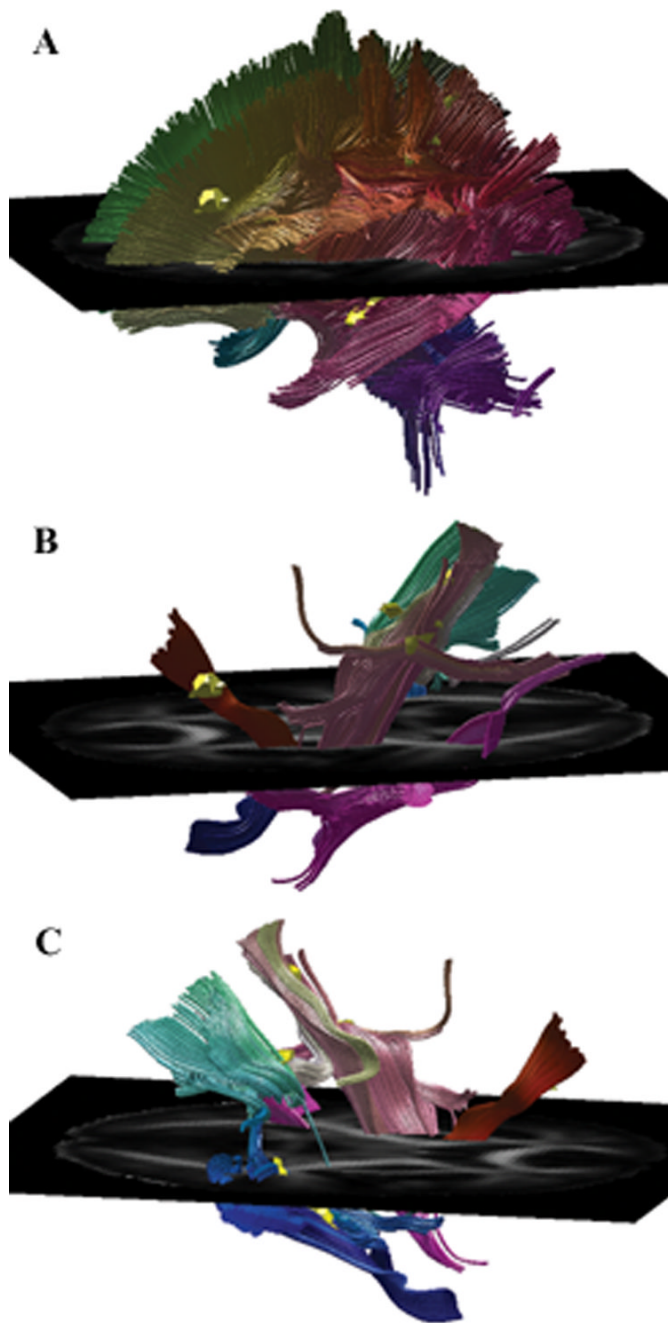
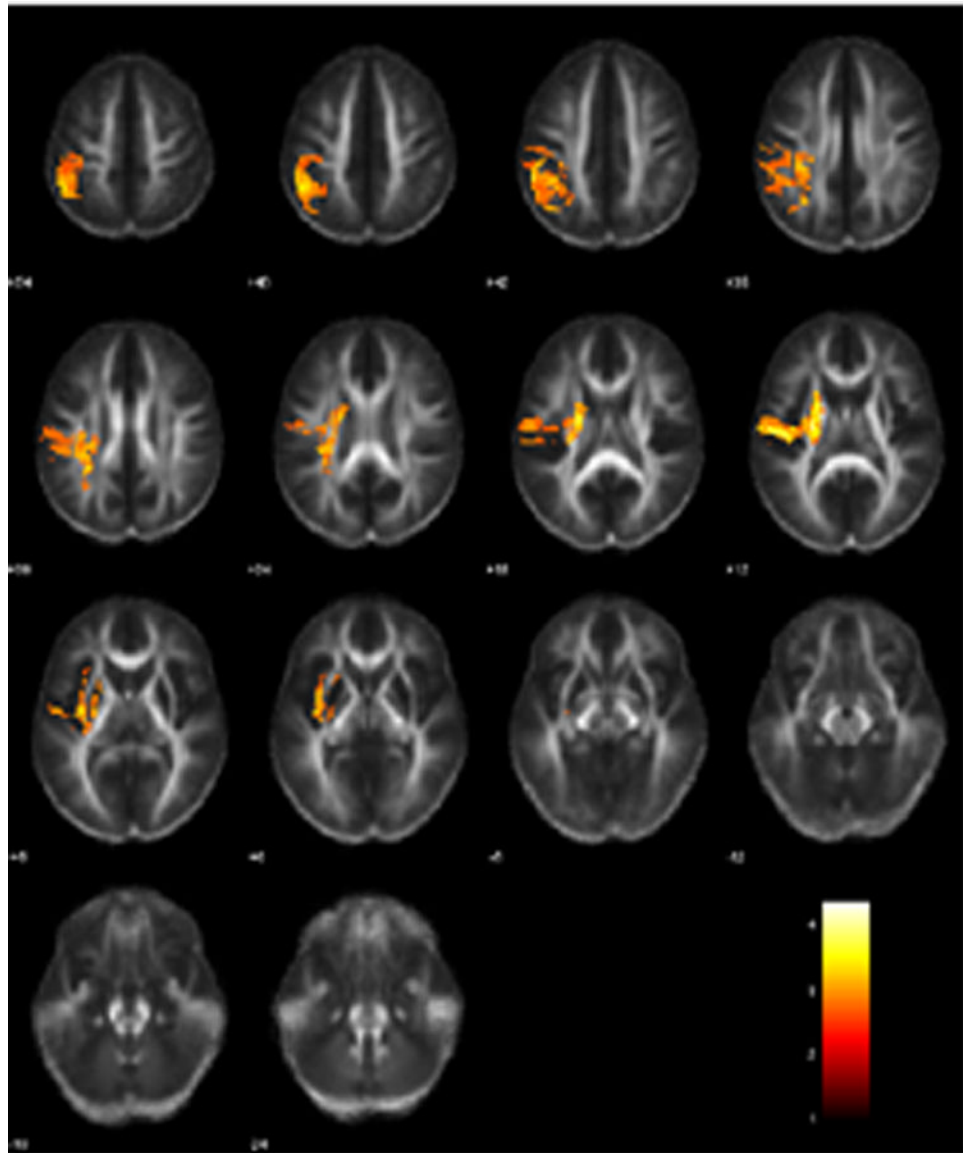


Figure 4.

White matter tracts associated with processing speed as determined by fiber tractography on group tensor map for healthy subjects. Regions of significant association between FA and processing speed, used as seed points, are shown in yellow. A. Whole brain fiber tracking on group average tensor map (azimuth and elevation angles of viewpoint = -104° and -11°). B. Tracts associated with left hemisphere regions of interest: left parietal (purple, superior longitudinal fasciculus, corona radiata), left temporal (red, inferior longitudinal fasciculus, inferior occipito-frontal fasciculus), left frontal (brown, fronto-striatal projections). C. Tracts associated with right hemisphere regions of interest: right parietal (turquoise, superior

longitudinal fasciculus, corona radiata), right temporal (blue, inferior longitudinal fasciculus, inferior occipito-frontal fasciculus). Fiber tractography results are rendered as streamtubes.



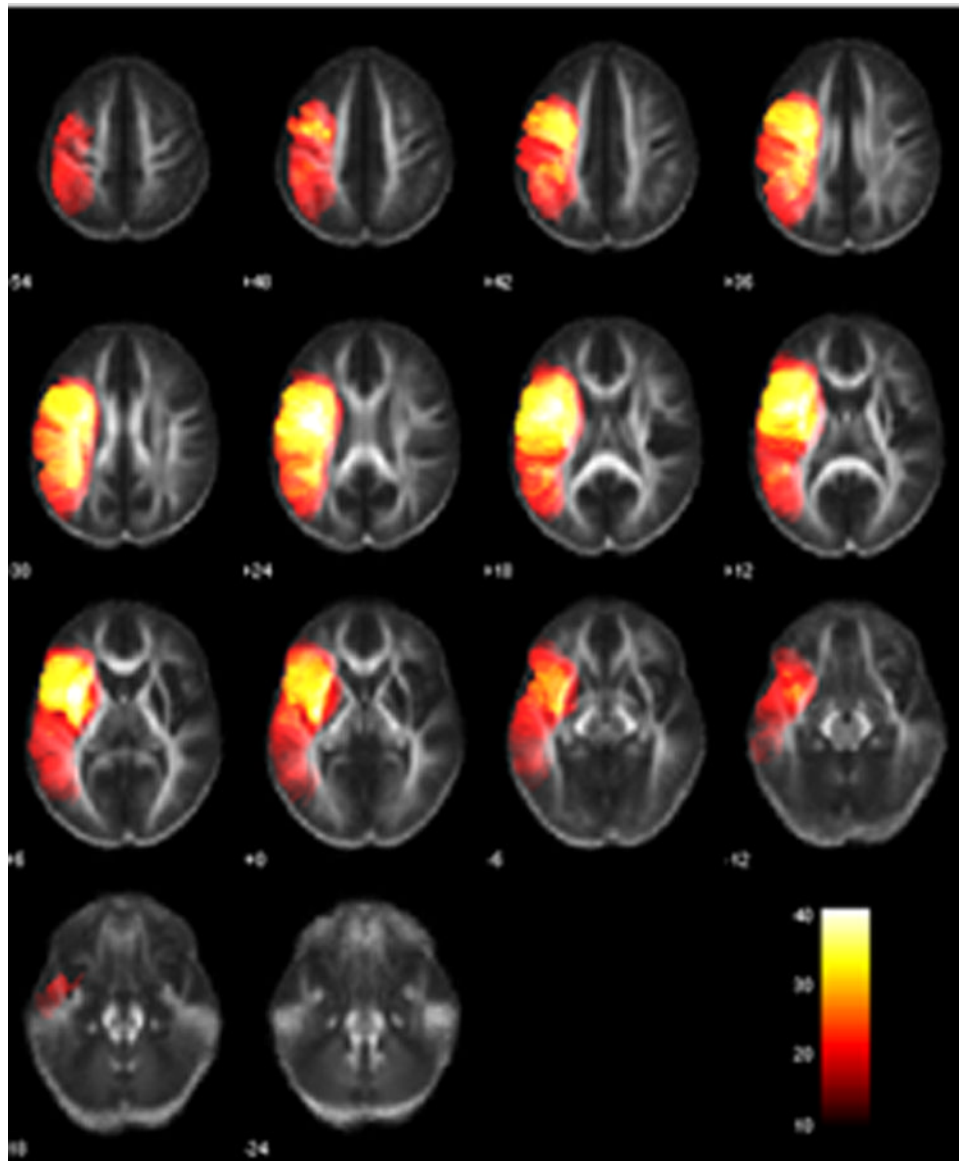


Figure 5.
A, B. Brain lesions associated with processing speed deficits in left-hemisphere stroke patients. Voxel-based lesion symptom mapping results have been overlaid on the mean FA image for young healthy subjects. A. Axial slices from superior ($z = 60$ mm, top left) to inferior ($z = -24$ mm, bottom right) sections. Lesions in parietal white matter and adjacent gray matter critical for processing speed can be seen on sections $z = 56$ to 24). Colorbar indicates t-values. B. Number of patients whose lesions overlap at each voxel, displayed on the same axial slices. Only voxels where at least 10 patients had lesions are include. The figure outlines the overall lesioned areas captured by the patient group, which is restricted by the boundaries of the vascular distributions that feed these areas.

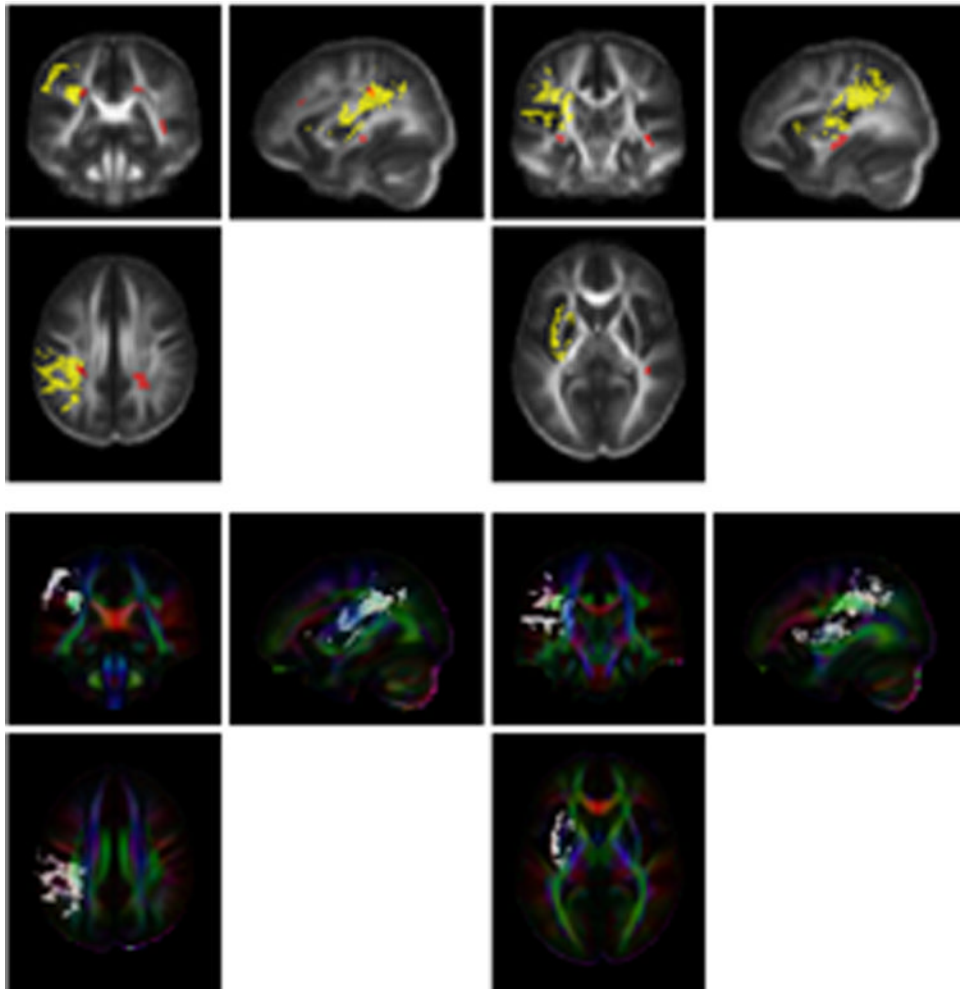


Figure 6.

Comparison of findings with VBM analysis based on DTI data from healthy subjects and VLSM analysis based on lesion data from left-hemisphere stroke patients. Top row: Voxel-based lesion symptom mapping (yellow) and voxel-based morphometry (red) results superimposed on mean FA image for healthy subjects. Bottom row: VLSM results rendered on the primary eigenvector direction map. Both methods indicate involvement of left parietal white matter. Consistent with the trajectory of superior longitudinal fasciculus, the parietal white matter lesions critical for processing speed cover a region with a strong anterior-posterior orientation. Cross-sections were taken at $x = -30$, $y = -35$, $z = 35$ mm (left column) and $x = -33$, $y = -22$, $z = -7$ mm (right column).

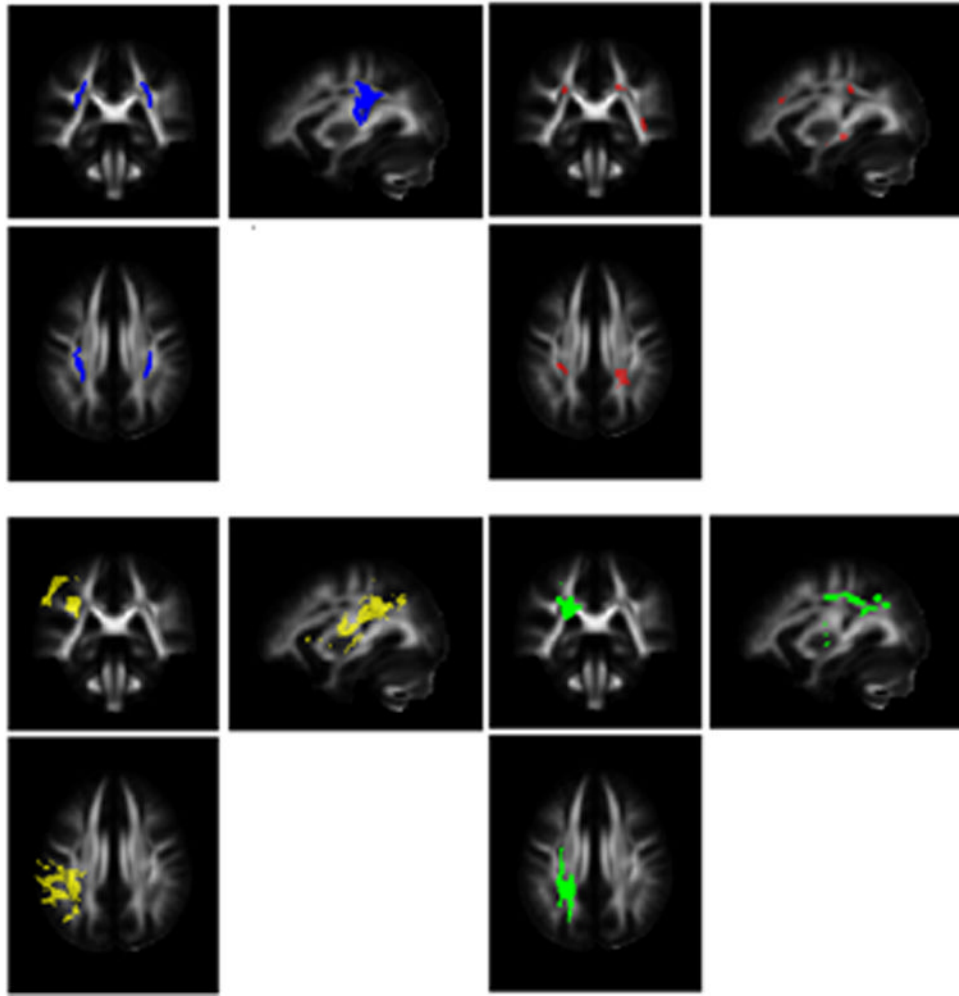


Figure 7.

Left superior longitudinal fasciculus and processing speed. Top left: Probabilistic map of core section of superior longitudinal fasciculus (Burgel et al., 2006), thresholded at 30% overlap, shown in blue. Top right: Regions showing positive association between fractional anisotropy and processing speed according to VBM analysis, shown in red. Bottom left: Regions showing an association between the presence of a brain lesion and impaired processing speed according to VLSM analysis, shown in yellow. Bottom right: Fiber tractography results with seed points selected from the voxel-based morphometry-defined region of interest in left parietal white matter. All images are overlaid on the group FA map for healthy subjects. Cross-sections were taken at $x = -30$, $y = -35$, $z = 35$ mm.

Table 1

Clusters of voxels showing significant correlations between FA and speed of processing, and coordinates of the voxels with peak significance levels. Effects of age, sex and total intracranial volume have been partialled out.

Anatomical extent of cluster, and associated tracts (putative)	Nearest cortical gray matter	MNI coordinates (X Y Z mm)	P-value at peak voxel	Z-score at peak voxel	Size
Left parietal lobe	BA 40	-28 -32 34	4.8×10^{-5}	3.90	74
<i>Superior longitudinal fasc.</i>		-22 -44 52	5.5×10^{-5}	3.87	
<i>Corona radiata (superior)</i>		-24 -40 42	0.0018	2.91	
Right parietal lobe	BA 40	20 -36 36	2.6×10^{-4}	3.47	95
<i>Superior longitudinal fasc.</i>		26 -44 36	6.4×10^{-4}	3.22	
<i>Corona radiata (superior)</i>		20 -50 40	0.0021	2.87	
Left middle frontal gyrus	BA 46	-24 32 26	5.9×10^{-6}	4.38	57
<i>Superior fronto-occipital fasc.</i>					
<i>Anterior thalamic radiation</i>					
<i>Extreme capsule</i>					
Left temporal lobe	BA 20, 48	-36 -14 -8	1.6×10^{-4}	3.60	77
<i>Inferior longitudinal fasc.</i>		-30 -24 -4	0.0015	2.97	
<i>Inferior occipito-frontal fasc.</i>					
<i>Uncinate fasc.</i>					
Right temporal lobe	BA 20, 21	42 -18 -4	8×10^{-7}	4.80	129
<i>Inferior longitudinal fasc.</i>		44 -26 -6	1.2×10^{-4}	3.67	
<i>Inferior occipito-frontal fasc.</i>		42 -32 6	3.5×10^{-4}	3.39	
<i>Optic radiation</i>					